Spectroscopy of CF_3COZ Compounds. V. Vibrational Spectra and Structure of Solid Trifluoroacetic Acid

C. V. Berney[1]

Contribution from the Air Force Rocket Propulsion Laboratory, Edwards, California 93523. *Received June 22, 1972*

Abstract: Infrared, Raman, and neutron-scattering data are correlated for solid CF_3COOH and CF_3COOD in the region 2000–200 cm^{-1}. Comparisons between liquid and solid CF_3COOH suggest that both phases are composed of hydrogen-bonded chains. Two possible structures are proposed, of which one (monoclinic, $P2/m$) is favored by the spectroscopic data. Vibrational assignment of CF_3COOH is straightforward, but that of CF_3COOD is more difficult; the normal modes in the region 910–610 cm^{-1} apparently change significantly on deuteration. Mixing between the O–D torsion and the O–C–O scissors mode implies a deviation from coplanarity of adjacent carboxyl groups. If this is actually the case, the symmetry of the (rigid) space group is reduced to $P2$. A solid–solid phase transition is observed at 220.5°K. Raman spectra taken above and below this temperature snow only small frequency differences and suggest that the transition involves a change in the orientation or relative motion of adjacent carboxyl groups.

This series of papers has dealt with vibrational assignments of molecules with the structure $CF_3C(=O)Z$, where the Z substituent has been Cl,[2a] CF_3,[2b] H,[3] and F.[4] In each case, the attractive forces between the individual molecules of the substance are small, and the material is a gas at room temperature. Although conclusions regarding the equilibrium conformation of $(CF_3)_2C=O$ were drawn from its vibrational spectrum in ref 2b, in most cases the structure of the molecular entity considered has been known from previous microwave[5] or electron-diffraction[6] studies.

The subject of the present work is trifluoroacetic acid, CF_3COOH. It is isoelectronic with trifluoroacetyl fluoride, but the redistribution of charges involved in replacing the –F with an –OH group profoundly changes the nature of the intermolecular forces; hydrogen bonds are formed, with the result that CF_3COOH is a liquid at room temperature. It freezes at −15°,[7] and the structure of the resulting solid has not been determined by crystallographic methods. The intimate connection between vibrational properties and structure makes it impossible to discuss the former without assuming a model for the latter. Thus the focus of the present study is on the structure of the material studied to a much larger extent than in the previous works.[2-4]

Structure of the Condensed Phases

Clague and Novak[8] have published a thorough study of the spectra of solid CF_3COOH and CF_3COOD. The lack of correspondence between many of the observed Raman and infrared frequencies led them to conclude that a center of symmetry was present; they further concluded that the solid is thus composed of hydrogen-bonded cyclic dimers rather than infinite chains. Formic[9] and acetic[10,11] acids contain such hydrogen-bonded chains in the solid state, both with space groups of $Pna2_1$ (C_{2v}^9).

Spectra taken in the course of the present study are in good agreement with those of ref 8, in particular with regard to the differences between the Raman and infrared frequencies. However, the conclusion to be drawn from these differences is not that the solid is associated in the form of dimers, but simply that the unit cell contains a center of symmetry. Two examples of chain structures meeting this requirement are shown in Figure 1. The first is $Pbca$ (D_{2h}^{15}); it consists of conventionally linked chains, with molecules in the upper chain related to those in the lower chain by the inversion center (Figure 1a). The basis for a second structure is shown in Figure 1b, with two chains facing each other to form one double chain or ribbon. The carbon and oxygen atoms of each ribbon will be approximately coplanar, and the angle formed by the planes of two adjacent parallel ribbons can be adjusted to satisfy packing requirements, giving a structure of space group $P2/m$ (C_{2h}^1) with four molecules per unit cell.

There is in fact a line of reasoning indicating that CF_3COOH in both the liquid and the solid is associated mainly in the form of chains. (a) The dielectric constant[12] of liquid CF_3COOH at 20° is 39.5. This is a very high value compared with that of CH_3COOH (6.15), which consists mostly of dimers in the liquid phase, but it is comparable with that of HCOOH (58.5), which is known to form chains.[13] The dielectric constant of CF_3COOH changes by almost a factor of 2 on going from −11 to 28°,[14] an observation which is easily explained if the liquid is composed of chains (whose average length would depend on the temperature), but is anomalous if the liquid is composed of dimers. In addition, Murty and Pitzer[15] have studied the infrared

(1) NRC Senior Research Associate, 1972–1973.
(2) (a) C. V. Berney, *Spectrochim. Acta*, 20, 1437 (1964); (b) *ibid.*, 21, 1809 (1965).
(3) C. V. Berney, *Spectrochim. Acta, Part A*, 25, 793 (1969).
(4) C. V. Berney, *ibid.*, 27, 663 (1971).
(5) R. C. Woods, *J. Chem. Phys.*, 46, 4789 (1967).
(6) G. A. Boulet, Ph.D. Thesis, University of Michigan, 1964; *Diss. Absir.*, 25, 3283 (1964).
(7) F. Swarts, *Bull. Sci. Acad. Roy. Belg.*, 8, 343 (1922); "Beilsteins Handbuch der Organischen Chemie," Springer-Verlag, Berlin, 1942, E II 2, p 186.
(8) D. Clague and A. Novak, *J. Chim. Phys.*, 67, 1126 (1970).
(9) F. Holtzberg, B. Post, and I. Fankuchen, *Acta Crystallogr.*, 6, 127 (1953).
(10) R. E. Jones and D. H. Templeton, *ibid.*, 11, 484 (1958).
(11) P.-G. Jönsson, *Acta Crystallogr., Sect. B*, 27, 893 (1971).
(12) A. A. Maryott and E. R. Smith, *Nat. Bur. Stand. (U. S.) Cir.*, 514 (1951).
(13) R. J. Jakobsen, Y. Mikawa, and J. W. Brasch, *Spectrochim. Acta, Part A*, 23, 2199 (1967).
(14) J. H. Simons and K. E. Lorentzen, *J. Amer. Chem. Soc.*, 72, 1426 (1950).
(15) T. S. S. R. Murty and K. S. Pitzer, *J. Phys. Chem.*, 73, 1426 (1969).

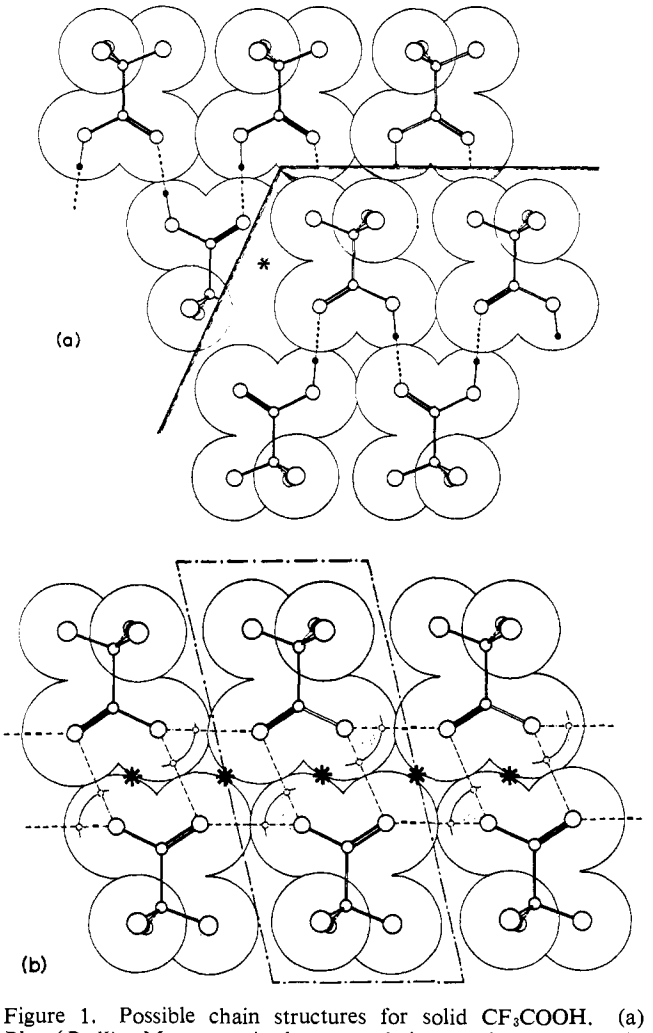

Figure 1. Possible chain structures for solid CF_3COOH. (a) *Pbca* (D_{2h}^{15}). Monomers in the upper chain are related to those in the lower chain by the inversion operation (asterisk). The unit cell contains two monomers (comprising a catemer) from each of the two chains. Hydrogen bonds are indicated by dashed lines. (b) *P2/m* (C_{2h}^{1}). The inversion relates monomers facing each other in the double chain, so that the catemer is structurally similar to the gas-phase dimer. The unit cell contains a catemer from the pictured chain (enclosed by dash-dotted lines) plus one from another chain parallel to it, but with the plane oriented at an angle determined by packing requirements. Spectroscopic evidence discussed in the text supports this model.

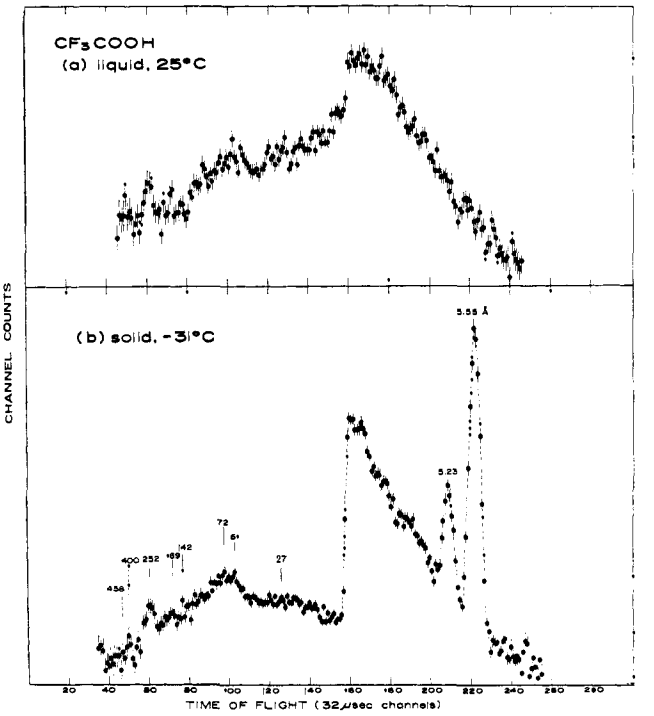

Figure 2. Neutron inelastic-scattering spectra of CF_3COOH. Wave number equivalents of some of the channels are indicated (458. . .27 cm^{-1}). Intense Bragg peaks are observed in the solid for neutron wavelengths of 5.23 and 5.55 Å; they can be interpreted as the 100 and 002 reflections of a monoclinic unit cell with parameters $a = 5.25$, $b = 9.165$, $c = 11.142$ Å, and $\beta = 85°$.

spectra of trifluoroacetic acid in nonpolar solvents and concluded that the association is primarily linear. (b) Neutron-scattering spectra of CF_3COOH have been obtained for both the liquid and the solid (Figure 2). The inelastic-scattering features (channels below ~160) stay remarkably constant over the phase change. Thus if the liquid consists of hydrogen-bonded chains, the solid must be similarly constructed.

Both of the structures under consideration (Figure 1) have unit cells containing four monomers, two each from neighboring chains. Adjacent monomers in a given chain are obviously more closely coupled than monomers in neighboring chains, and it will be convenient to have a specific term for such a vibrational entity. We suggest *catemer* (Latin *catena*, chain), which can be generally defined as that sequence of monomers in a chain which are related by symmetry elements other than simple translation. The factor group of the catemer in the *Pbca* (orthorhombic) structure is C_{2v} and the representation of the internal vibrations is

$$\Gamma_{int}(C_{2v}) = 12a_1 + 6a_2 + 12b_1 + 6b_2$$

where the a_1, b_1, and b_2 vibrations are infrared active and all the vibrations are Raman active. If the monomer is regarded as belonging to the point group C_s, the *Pbca* model predicts that all modes in the solid originating as a′ vibrations in the monomer will be split by catemeric coupling in the infrared and that all modes will be split in the Raman.

In the *P2/m* (monoclinic) model, the factor group of the catemer is C_{2h}, and the representation of the internal vibrations is

$$\Gamma_{int}(C_{2h}) = 12a_g + 6b_g + 6a_u + 12b_u$$

In this case, the principle of mutual exclusion holds within the catemer; in-phase vibrations of the two monomers are a_g or b_g and Raman active, while out-of-phase modes are a_u or b_u and infrared-active. The only splitting observed using this model will be due to interchain coupling.

With the exception of the O–H(D) stretches and CF_3 torsions, all of the internal vibrations of CF_3COOH and CF_3COOD are found between 1900 and 200 cm^{-1}. Spectra for these two species are given in Figures 3 and 4. Although evaluation of the amount of splitting present is complicated by numerous instances of Fermi resonance, it is clear that the overall pattern is more in accord with $\Gamma_{int}(C_{2h})$ than with $\Gamma_{int}(C_{2v})$. In particular, the large difference between the position of the C=O stretch in the Raman (1706 cm^{-1}) and the infrared (1763 cm^{-1}) suggests a catemeric center of symmetry, as does the lack of splitting in most of the sharp peaks.

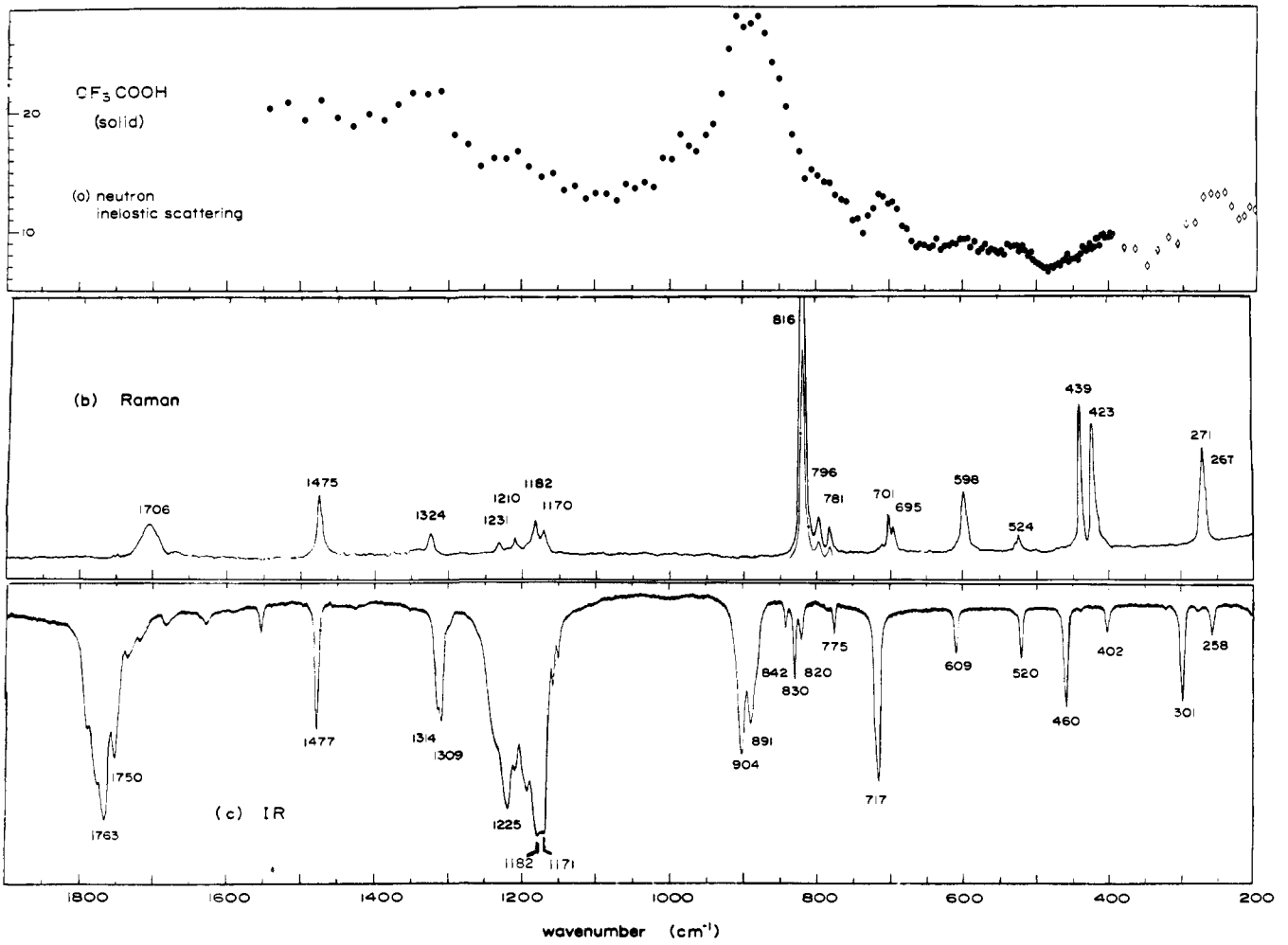

Figure 3. Spectra of solid CF_3COOH. (a) Neutron inelastic-scattering spectrum. Data of Collins and Haywood[19] are plotted with black dots (ordinate represents percentage of monitor counts). Diamond-shaped points are the data of Figure 2b, linearly scaled to match at 398 cm^{-1}. (b) Raman spectrum. (c) Infrared spectrum.

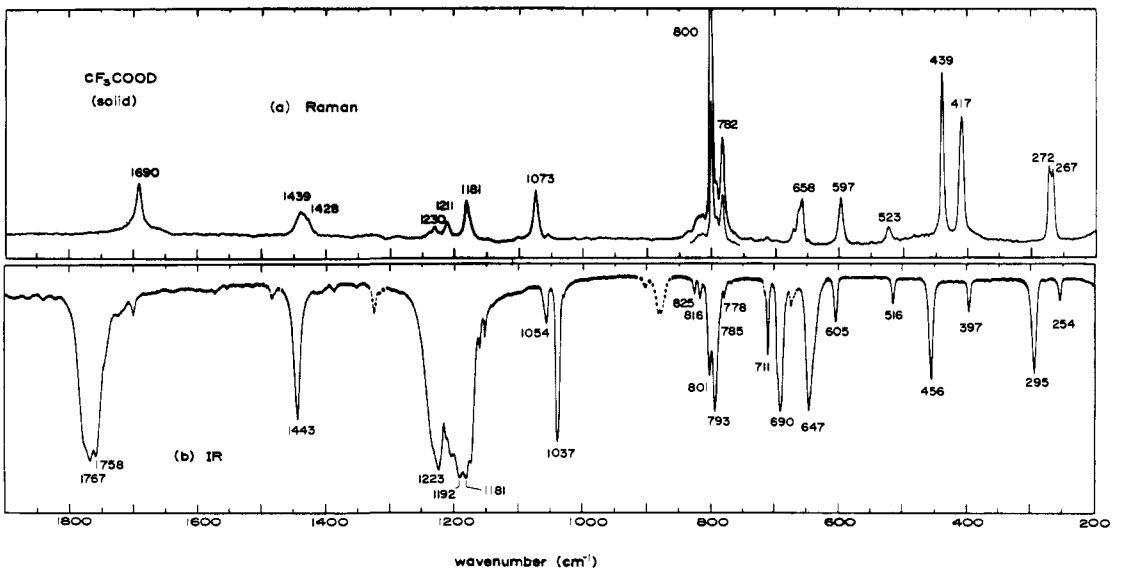

Figure 4. Spectra of solid CF_3COOD. (a) Raman spectrum. (b) Infrared spectrum. Peaks due to CF_3COOH are indicated by a dashed line.

Thus the $P2/m$ structure is favored by the spectroscopic evidence and will be assumed to be correct throughout the rest of this paper. In this case, the catemer is structurally similar to the cyclic dimer found in the gas phase. The present study is thus in essential agreement with the spectroscopic analysis given by Clague and

Novak,[8] differing mainly in that their use of the term *dimer* seems to exclude a chain structure.

The *P2/m* model illustrated in Figure 1b has equal distances between the carbonyl and hydroxyl oxygen atoms in the same catemer and those in adjacent catemers; this is a result of the assumed spherical nature of the van der Waals potential surfaces rather than the presence of any formal symmetry element. It suggests that the hydrogen bonds in solid CF_3COOH may be bifurcated, a situation which is unusual but not unprecedented.[16] It would be interesting to have definitive results (*e.g.*, from a neutron-diffraction investigation) to clear up this point.

Experimental Section

The spectra displayed in Figure 2 were obtained on a time of flight spectrometer at the Army Materials and Mechanics Research Center, Watertown, Mass.; this type of instrument has been previously described in the literature.[17,18] Figure 3a shows neutron-scattering data obtained by Collins and Haywood[19] using a spectrometer measuring energy loss rather than energy gain. This instrument extends the useful range of observation to ~1400 cm^{-1} or more, providing much more information on the internal modes of the molecule and allowing more detailed comparison with the Raman and infrared spectra.

Raman spectra of CF_3COOH (Figure 3b) and CF_3COOD (Figure 4a) were run using the 5145-Å line of an Ar^+ laser at ~600 mW and a Spex monochromator.[20] The samples were placed in glass tubes and mounted in an unsilvered Dewar which was then cooled with boil-off from a supply of liquid nitrogen. The temperature of the solid was not closely controlled and ranged from 258°K (the freezing point) to about 210°K. The spectra were calibrated with Ar emission lines.[21,22]

A conventional liquid-nitrogen cold cell[23] was used in running the infrared spectra (Figures 3c and 4b). Both outer windows and the cold window were CsI. Samples were deposited from the vapor state and annealed by repeated warming and recooling. The temperature of the sample as the spectra were run was about 106°K. Calibration was carried out using the absorption lines of atmospheric water vapor.[24] The instrument used was a Beckman IR-12. Resolution and frequency accuracy for the optical spectra reported here are within 2 cm^{-1}.

The CF_3COOH used in the Raman experiments was obtained from Pierce Chemical, Rockford, Ill., and was labeled "99+% pure." The CF_3COOD was from Bio-Rad Laboratories, Richmond, Calif.; the isotopic composition was given as 99 atom % D. Samples used in the infrared experiments were from Eastman Organic Chemicals, Rochester, N. Y., and an older specimen of CF_3COOD from Bio-Rad labeled 98 atom % D. Additional infrared experiments with mixtures of varying isotopic composition were carried out to identify features due to CF_3COOH in CF_3COOD.

A differential thermal analysis experiment was carried out on CF_3COOH using a Du Pont Model 900 instrument equipped with a differential scanning calorimeter cell. The sample was initially cooled to 173°K with liquid nitrogen and then was heated at 5°/min. Two endothermic peaks were found, a weak one at 220.5°K and a strong one at 257.9°K. The latter corresponds to melting of the sample, so the former must represent a solid-solid phase transition. This observation immediately raises the question of whether the Raman spectra of Figures 3b and 4a (for the most part taken above 220°K) can properly be compared with the infrared spectra of Figures 3c and 4b (taken at ~106°K). Fortunately, the Raman spectra of ref 8 were taken at ~77°K, and the agreement between the two sets of observations indicates that the comparison remains valid. Frequency differences average less than 2 cm^{-1}, well within the combined error limits. The largest discrepancies occur for ν_{C-O} (1475 *vs.* 1482[8] for CF_3COOH, 1439 *vs.* 1444[8] for CF_3COOD) and for δ_{COH} (1324 *vs.* 1330[8] and 1073 *vs.* 1076[8]).

Vibrational Assignment

CF_3COOH. Assignments for the fundamental frequencies of solid CF_3COOH are given in Table I, together with infrared frequencies for the cyclic dimers from the matrix-isolation work of Redington and Lin.[25] The descriptive notation follows the usage of ref 4 and 25. Particularly above 1000 cm^{-1}, there is a close correspondence between the frequencies of the solid and dimer; since clear arguments for the assignment of $\nu_{C=O}$, ν_{C-O}, δ_{COH}, and the C—F stretching vibrations are given in ref 8 and 25, they will not be repeated here.

Table I. Fundamental Frequencies of CF_3COOH (Cyclic Dimer and Solid)

Description	Cyclic dimer[a] Ir, Ne matrix	Solid Ir	Solid Raman
ν_{OH}	2922	2918	
$\nu_{C=O}$	1786	1763	1706
ν_{C-O}	1475	1477	1475
δ_{COH}	1318	1314	1324
		1309	
ν_{FCF_2}	1244	1225	1231
ν_{FCF}	1197	1196	1210
ν_{CF_3}	1178	1182	1182
		1171	
τ_{OH}	927	904	[~875][c]
		891	
ν_{CC}	828	830	816
δ_{CF_3}	686	775	781
δ_{OCO}	712	717	701
δ_{FCF_2}	607[b]	609	598
δ_{FCF}	520[b]	520	524
$\omega_{antigear}$	459	460	439
$\rho_{antigear}$	390	402	423
ω_{gear}	240	301	272
ρ_{gear}	240	258	267
τ_{CF_3}		[~27 ?][c]	[~27 ?][c]

[a] Table 4, ref 25. [b] Interchanged from Table 4, ref 25, but in agreement with the text. [c] From neutron-scattering measurements.

Consideration of neutron-scattering data in conjunction with infrared and Raman spectra can lead to a considerable increase in the certainty of the analysis since the neutron scattering is especially sensitive to motions of ^1H nuclei.[26] Figure 3a depicts the neutron-scattering spectrum of CF_3COOH as observed by Collins and Haywood,[19] with additional data from experiments carried out by the present author. The spectrum is dominated by the intense doublet around 900 cm^{-1}, which must be the torsional motion of the hydroxyl group, τ_{OH}. The splitting is probably due to frequency differences between the *gerade* and *ungerade* modes, since the lower-frequency peak (~875 cm^{-1}) is below the corresponding infrared feature (904, 891 cm^{-1}). The splitting in the infrared must be due to interchain

(16) W. C. Hamilton and J. A. Ibers, "Hydrogen Bonding in Solids," W. A. Benjamin, New York, N. Y., 1968, p 211.
(17) D. J. Hughes, H. Palevsky, W. Kley, and E. Tunkelo, *Phys. Rev.*, **119**, 872 (1960).
(18) K. E. Larson, U. Dahlborg, S. Holmryd, K. Othes, and R. Stedman, *Ark. Fys.*, **19**, 199 (1959).
(19) M. F. Collins and B. C. Haywood, *J. Chem. Phys.*, **52**, 5740 (1970).
(20) R. E. Miller, D. L. Rousseau, and G. E. Leroi, Technical Report No. 22, ONR Contract 1858 (27), May 1967; DDC Accession No. AD651646.
(21) "American Institute of Physics Handbook," McGraw-Hill, New York, N. Y., 1957, p 7-59.
(22) L. Minnhagen, *Ark. Fys.*, **25**, 203 (1963).
(23) E. L. Wagner and D. F. Hornig, *J. Chem. Phys.*, **18**, 296 (1950).
(24) "IUPAC Tables of Wavenumbers for the Calibration of Infrared Spectrometers," Butterworths, Washington, D. C., 1961.
(25) R. L. Redington and K. C. Lin, *Spectrochim. Acta, Part A*, **27**, 2445 (1971).
(26) B. K. Aldred, R. C. Eden, and J. W. White, *Discuss. Faraday Soc.*, **No. 43**, 169 (1967).

Table II. Infrared and Raman Spectra of Solid CF_3COOH (2000–200 cm^{-1})

Infrared[a]		Raman		
ν, cm^{-1}	Inten	$\Delta\nu$, cm^{-1}	Rel peak height	Assignment[b]
~1860	vw			
1834	vw			$\nu^{g}_{FCF_2} + \delta^{u}_{FCF_2}$ (1231 + 609 = 1840)
1786 sh	w			$\delta^{g}_{COH} + \omega^{u}_{antigear}$ (1324 + 460 = 1784)
1774 sh	w			$\nu^{g}_{C-O} + \omega^{u}_{gear}$ (1475 + 301 = 1776)
1763	vs			$\nu^{u}_{C=O}$
1750	m			$\nu^{g}_{FCF_2} + \delta^{u}_{FCF}$ (1231 + 520 = 1751)
1733	w			
1722	w			
		~1720 sh	~3	$\delta^{u}_{COH} + \rho^{u}_{antigear}$ (1309 + 402 = 1711)
		1706	7	$\nu^{g}_{C=O}$
		~1690 sh	~4	$\nu^{g}_{CF_3} + \delta^{g}_{FCF}$ (1182 + 524 = 1706)
1680	mw			$\nu^{g}_{FCF_2} + \omega^{u}_{antigear}$ (1231 + 460 = 1691)
1627	mw			$\nu^{g}_{FCF_2} + \rho^{u}_{antigear}$ (1231 + 402 = 1633)
~1590	vw			$\delta^{g}_{OCO} + \tau^{u}_{OH}$ (701 + 904 = 1605)
1553	m			$\delta^{g}_{CF_3} + \delta^{u}_{CF_3}$ (781 + 775 = 1556)
1477	s			ν^{u}_{C-O}
		1475	14	ν^{g}_{C-O}
1432	vw			$\nu^{g}_{CF_3} + \rho^{u}_{gear}$ (1182 + 258 = 1440)
		1324	5	δ^{g}_{COH}
1314 1309	s			δ^{u}_{COH}
1296 sh	w			
		1231	3	$\nu^{g}_{FCF_2}$
1225	vs			$\nu^{u}_{FCF_2}$
		1210	3	ν^{g}_{FCF}
1208	w			$\delta^{g}_{FCF_2} + \delta^{u}_{FCF_2}$ (598 + 609 = 1207)
1196	m			ν^{u}_{FCF}
		1182	8	$\nu^{g}_{CF_3}$
		1170	6	$\delta^{u}_{CF_3} + \rho^{u}_{antigear}$ (775 + 402 = 1177)
1182 1171	vs			$\nu^{u}_{CF_3}$ $\delta^{g}_{CF_3} + \rho^{u}_{antigear}$ (781 + 402 = 1183)
1156	w			ν_{CF_3} ($CF_3{}^{13}COOH$)
1149	w			ν_{CF_3} ($^{13}CF_3COOH$)
904 891	s			τ^{u}_{OH}
880 sh				
842	m			$\omega^{g}_{antigear} + \rho^{u}_{antigear}$ (439 + 402 = 841)
830	ms			ν^{u}_{CC}
820	m			$\rho^{g}_{antigear} + \rho^{u}_{antigear}$ (423 + 402 = 825)
		816	100	ν^{g}_{CC}
		796	9	$2\rho^{u}_{antigear}$ (2 × 402 = 804)
		781	6	$\delta^{g}_{CF_3}$
775	m			$\delta^{u}_{CF_3}$
717	s			δ^{u}_{OCO}
		711	2	$\omega^{g}_{antigear} + \omega^{g}_{gear}$ (439 + 271 = 710)
		701	9	δ^{g}_{OCO}
		695	6	$\delta^{g}_{antigear} + \omega^{g}_{gear}$ (423 + 271 = 694)
609	m			$\delta^{u}_{FCF_2}$
		598	14	$\delta^{g}_{FCF_2}$
		528 sh	2	$2\rho^{g}_{gear}$ (2 × 267 = 534)
		524	3	δ^{g}_{FCF}
520	m			δ^{u}_{FCF}
460	ms			$\omega^{u}_{antigear}$
		439	33	$\omega^{g}_{antigear}$
		423	30	$\rho^{g}_{antigear}$
402	m			$\rho^{u}_{antigear}$
301	ms			ω^{u}_{gear}
		271	23	ω^{g}_{gear}
		267 sh	~12	ρ^{g}_{gear}
258	m			ρ^{u}_{gear}

[a] sh = shoulder; v, w, m, s = very, weak, medium, strong. [b] In many cases, more than one combination is available to explain a given peak. To save space, only one of the possibilities (usually chosen on the basis of likelihood of coupling) is given here.

coupling, since all ir-active modes are ungerade. With the possible exception of ν_{CF_3} (for which an alternate explanation in terms of Fermi-resonant combinations is available), the only modes which exhibit interchain coupling are those which involve large-amplitude motions of the hydrogen atom.

Another vibrational mode which must involve the hydrogen atom is δ_{OCO}, the scissors deformation of the carboxyl group. The presence of a moderately strong peak in the neutron-scattering spectrum around 700 cm^{-1} leads to the association of this mode with the Raman peak at 701 cm^{-1} and the strong infrared peak at 717 cm^{-1}.

The carbon–carbon stretching mode (strongly coupled with the symmetric C–F stretching vibration) is easily identified by its intensity in the Raman spectrum (Figure

3b). The corresponding infrared feature is a distinctive triplet (842, 830, 820 cm^{-1}) in which the outer members can be assigned to combinations (Table II). The only other fundamental expected to fall in this region is the trifluoromethyl umbrella deformation, δ_{CF_3}. This is evidently the sharp peak at 775 cm^{-1} in the infrared. If it is identified with the 781-cm^{-1} feature in the Raman spectrum, the 796-cm^{-1} peak can be explained as the overtone of the 402-cm^{-1} mode. This assignment puts δ_{CF_3} abve δ_{OCO}, contrary to the corresponding assignments for CF_3CFO[4] (δ_{OCF} = 761, δ_{CF_3} = 692 cm^{-1}), for monomeric CF_3COOH[25] (δ_{OCO} = 781, δ_{CF_3} = 663 cm^{-1}) and, to a smaller extent, for the ungerade vibrations of the dimer[25] (δ_{OCO} = 712, δ_{CF_3} = 686 cm^{-1}). The reduction of the separation between the two modes (from 118 to 26 cm^{-1}) as the dimer is formed shows that these vibrations (especially δ_{OCO}) are association-sensitive; since the solid is even more strongly associated than the dimer, further changes in position are not unreasonable. It should also be noted that the modes labeled ν_{CF_3}, ν_{CC}, δ_{OCO}, and δ_{CF_3} all imply a large component of motion along the C–C bond and thus will all interact strongly. The actual normal coordinates may differ widely from compound to compound.

The other assignments in the 700–200 cm^{-1} region follow readily from comparison with other CF_3COZ molecules.[3,4] The similarity between CF_3COOH and CF_3CFO[4] with regard to frequencies and relative intensities in both the Raman and the infrared is particularly striking.

CF_3COOD. The incoherent scattering cross section of the deuteron is an order of magnitude smaller than that of the proton, and the neutron scattering of CF_3COOD has not been studied. Thus our main tool in analyzing the Raman and infrared spectra of CF_3COOD (Figure 4) will be comparison with CF_3COOH. Except for the movement of δ_{COH} from 1324 to 1073 cm^{-1}, the pattern of Raman-active vibrations is virtually unchanged on deuteration. Accordingly, we assign peaks at 800, 782, 658, and 597 cm^{-1} to ν^g_{CC}, $\delta^g_{CF_3}$, δ^g_{OCO}, and $\delta^g_{FCF_2}$ (where the superscript g is used to distinguish the gerade mode of the catemer from its infrared-active counterpart).

Most of the absorptions in the infrared spectrum (Figure 4b) are also easily assigned. The C–F stretching region (1250–1150 cm^{-1}) is almost exactly the same as for CF_3COOH. The peak at 1037 cm^{-1} is obviously the COD deformation. Below 610 cm^{-1} we again have a pattern virtually identical to that found in CF_3COOH, and the same assignments can be made (Table III). It is in the region 910–610 cm^{-1} that the pattern changes drastically and a firm assignment becomes correspondingly difficult.

The four fundamentals expected to occur in this region are ν_{CC}, τ_{OD}, δ_{CF_3}, and δ_{OCO} (superscript u understood). The first of these can be identified with the doublet at 825, 816 cm^{-1} [where the doubling is explained as Fermi resonance with $\delta^g_{FCF} + \omega^u_{gear}$ (523 + 285 = 818) or $\rho^g_{antigear} + \rho^u_{antigear}$ (417 + 397 = 814)]. The sharp, weak peaks at 785 and 778 cm^{-1} have plausible explanations as combinations (Table IV), so we now have three fundamental modes to distribute among the four major features (801–793, 711, 690, and 647 cm^{-1}) in this region.

The 690- and 647-cm^{-1} peaks are of equivalent width and intensity, and the natural way to make the number of modes and features come out even is to attribute these two peaks to the same fundamental, split either by Fermi resonance or by an unusual amount of interchain coupling. All possible assignments in this region can now be described by the six permutations of the symbols (τ_{OD}, δ_{CF_3}, δ_{OCO}) or (1 2 3).

The most straightforward assignment is the one designated (1 2 3) above. The 801, 793 cm^{-1} feature is similar in intensity and appearance to τ_{OH} (904, 891) in CF_3COOH, though not so broad. The 711-cm^{-1} peak is as narrow as δ_{CF_3} (775) in CF_3COOH, though more intense. The intensity of each component of the 690, 647 doublet is similar to that of δ_{OCO} (717) in CF_3COOH. However, there is one major objection to this assignment: it implies a frequency ratio τ_{OH}/τ_{OD} of 1.14, much smaller than the value of 1.3–1.4 expected for this quantity. In addition, it raises the questions of why the δ_{OCO} mode is split so grossly in CF_3COOD and not in CF_3COOH and why $\delta^g_{CF_3} - \delta^u_{CF_3}$ increases from 6 to 71 cm^{-1} on deuteration. It will evidently be worth our while to examine the other assignments.

(1 3 2) parallels the frequency order of the assignment made by Redington and Lin[25] for cyclic CF_3COOD dimers, but it requires us to believe that the mode producing the sharp, moderately weak singlet at 775 cm^{-1} in CF_3COOH gives rise to the broad, intense doublet at 690, 647 cm^{-1} in CF_3COOD, and can thus be rejected. Assignments (2 1 3) and (3 1 2) both identify the sharp singlet at 711 cm^{-1} as τ_{OD}, which again strains credulity.

We are now left with (2 3 1) and (3 2 1). Both assign the 690, 647 doublet as τ_{OD}, giving an isotopic frequency ratio of 1.35, in the middle of the expected range. Since τ_{OD} probably involves the largest amplitudes of any of the three vibrations being considered, these assignments ease the burden of explaining the gross splitting. (Even if Fermi resonance is invoked, large anharmonic terms in the potential function are required to produce the amount of mixing observed.) The former assignment minimizes $\delta^g_{CF_3} - \delta^u_{CF_3}$ and $\delta^g_{OCO} - \delta^u_{OCO}$ but is

Table III. Fundamental Frequencies of CF_3COOD (Cyclic Dimer and Solid)

Description	Cyclic dimer[a] Ir, Ar matrix	Solid Ir	Solid Raman
ν_{OD}	2254	2241	2052
$\nu_{C=O}$	1780	1767	1690
ν_{C-O}	1435	1443	1439
ν_{FCF_2}	1243	1223	1230
ν_{FCF}	1192	1205	1211
ν_{CF_3}	1178	1192	1181
		1181	
δ_{COD}	1042	1037	1073
ν_{CC}	817	825	800
δ_{CF_3}	682	711	782
δ_{OCO}	706	801	658
		793	
τ_{OD}	800	690	
		647	
δ_{FCF_2}	603[b]	605	597
δ_{FCF}	502[b]	516	523
$\omega_{antigear}$	455	456	439
$\rho_{antigear}$	[390][c]	397	417
ω_{gear}	[240][c]	295	272
ρ_{gear}	[240][c]	254	267

[a] Table 4, ref 25. [b] Interchanged from Table 4, ref 25, but in agreement with the text. [c] $(CF_3COOH)_2$ value.

Table IV. Infrared and Raman Spectra of Solid CF_3COOD (2000–200 cm^{-1})

Infrared[a]		Raman		
ν, cm^{-1}	Inten	$\Delta\nu$, cm^{-1}	Rel peak ht	Assignment[b]
1987	vw			$\nu^{g}_{CC} + \nu^{u}_{CF_3}$ (800 + 1192 = 1992)
1882	vw			$\omega^{g}_{antigear} + \nu^{u}_{CO}$ (439 + 1443 = 1882)
1863	vw			$\rho^{g}_{antigear} + \nu^{u}_{C-O}$ (417 + 1443 = 1860)
1839	vw			$\nu^{g}_{CC} + \delta^{u}_{COD}$ (800 + 1037 = 1837)
1819	vw			$\delta^{g}_{CF_3} + \delta^{u}_{COD}$ (782 + 1037 = 1819)
~1777 sh	w			$\delta^{g}_{FCF_2} + \nu^{u}_{CF_3}$ (597 + 1187 = 1784)
1767	vs			$\nu^{u}_{C=O}$
1758	s			δ^{g}_{COD} + [690] (1073 + 690 = 1763)
~1744 sh	w			$\nu_{FCF_2} + \delta_{FCF}$ (1230 + 516 = 1223 + 523)
1722	w			$\nu_{C-O} + \omega^{u}_{gear}$ (1439 + 295 = 1734)
1699	mw			$\rho^{g}_{gear} + \nu^{u}_{C-O}$ (267 + 1433 = 1710)
		1690	11	$\nu^{g}_{C=O}$
1571	vw			$\nu^{g}_{CF_3} + \rho^{u}_{antigear}$ (1181 + 397 = 1578)
1552	vw			$\delta^{g}_{FCF} + \delta_{COD}$ (523 + 1037 = 1560)
1483	mw			ν_{C-O} (CF_3COOH)
1443	s			ν^{u}_{C-O}
		1439	6	ν^{g}_{C-O}
		1428 sh	~4	$\delta^{u}_{COD} + \rho^{u}_{antigear}$ (1037 + 397 = 1434)
1405	vw			$\nu^{g}_{CC} + \delta^{u}_{FCF_2}$ (800 + 605 = 1405)
1385	w			$\delta^{g}_{FCF_2} + \delta^{u}_{OCO}$ (597 + 793 = 1390)
1351	vw			$\delta^{g}_{FCF} + \nu^{u}_{CC}$ (523 + 825 = 1348)
1323	mw			δ_{COH} (CF_3COOH)
1314	vw			δ^{u}_{COH} ($CF_3COOH)_2$
		1237	1	$\nu^{g}_{CC} + \omega^{g}_{antigear}$ (800 + 439 = 1239)
		1230	2	$\nu^{g}_{FCF_2}$
1223	vs			$\nu^{u}_{FCF_2}$
1212 sh	w			$\rho^{g}_{antigear} + \delta^{u}_{OCO}$ (417 + 793 = 1210)
		1211	3	ν^{g}_{FCF}
1205	m			ν^{u}_{FCF}
1192 1181	vs			$\nu^{u}_{CF_3}$
1173 sh				
		1181	12	$\nu^{g}_{CF_3}$
1159	w			ν_{CF_3} ($CF_3{}^{13}COOD$)
1151	w			ν_{CF_3} ($^{13}CF_3COOD$)
		1073	10	δ^{g}_{COD}
		1053	1	$\omega^{u}_{antigear} + \delta^{u}_{FCF_2}$ (456 + 605 = 1061)
1054	m			$\delta^{g}_{OCO} + \rho^{u}_{antigear}$ (658 + 397 = 1055)
1037	s			δ^{u}_{COD}
1027	vw			
902	w			τ_{OH} ($CF_3COOH)_2$
882 876	m			τ_{OH} (CF_3COOH)
825	mw	821[c]	3	ν^{u}_{CC}
816	mw	814[c]	2	$\delta^{g}_{antigear} + \rho^{u}_{antigear}$ (417 + 397 = 814)
		800	70	ν^{g}_{CC}
		792 sh	~12	$2\rho^{u}_{antigear}$ (2 × 397 = 794)
		782	21	$\delta^{g}_{CF_3}$
801 793	s			δ^{u}_{OCO}
785 sh	w			$\omega^{g}_{gear} + \delta^{u}_{FCF}$ (272 + 516 = 788)
778	w			$\rho^{g}_{gear} + \delta^{u}_{FCF}$ (267 + 516 = 783)
768	vw			$\delta^{g}_{FCF} + \rho^{u}_{gear}$ (523 + 254 = 777)
716 sh	vw	708	1	δ_{OCO} (CF_3COOH)
711	ms			$\delta^{u}_{CF_3}$
690	s			$\omega^{g}_{gear} + \rho^{u}_{antigear}$ (272 + 397 = 669) in resonance with τ_{OD}
674[c]	mw			
		671	3	
		663	~18	
		658	12	δ^{g}_{OCO}
647	s			τ_{OD} in resonance with $\omega^{g}_{gear} + \rho^{u}_{antigear}$
605	ms			$\delta^{u}_{FCF_2}$
		597	12	$\delta^{g}_{FCF_2}$
		523	4	δ^{g}_{FCF}
516	m			δ^{u}_{FCF}
456	s			$\omega^{u}_{antigear}$
		439	41	$\omega^{g}_{antigear}$
		417	30	$\rho^{g}_{antigear}$
397	m			$\rho^{u}_{antigear}$
295	s			ω^{u}_{gear}
		272	18	ω^{g}_{gear}
		267	17	ρ^{g}_{gear}
254	m			ρ^{u}_{gear}

[a] sh = shoulder; v, w, m, s = very, weak, medium, strong. [b] Assignment (3 2 1) in the region 910–610 cm^{-1} is used here for convenience. See text, p 713. [c] Vibration due to mixed catemer ($CF_3COOD \cdot CF_3COOH$).

difficult to rationalize with regard to shapes and intensities, while the latter, (3 2 1), does the opposite.

We are left with the feeling that none of the proposed assignments can by itself give a completely satisfactory account of the observed spectrum. Evidently deuteration induces a considerable redistribution of internal coordinates among the normal coordinates of all three vibrations in this region. This conclusion is particularly interesting in that it implies mixing between τ_{OD} and δ_{OCO}, which could not occur if the catemer contained a plane of symmetry.

Redington and Lin[25] have concluded that the CF_3 group in the matrix-isolated CF_3COOH momomer is twisted by perhaps 10–20° out of the skeletal plane. This twist formally changes the point group from C_s to C_1, but it seems insufficient to account for significant coupling between τ_{OD} and δ_{OCO} in the solid, since the CF_3 group retains approximate local threefold symmetry and is thus dynamically isotropic, as well as being physically distant from the carboxyl group. A more direct coupling between the torsion and the scissors mode would arise if the two carboxyl groups within the catemer were not strictly coplanar, but were overlapped or puckered in the manner suggested in Figure 1b. This change nominally reduces the catemeric factor group to C_2 and the space group to $P2$ (monoclinic), but the distortion from $P2/m$ need not be large. In addition, the barrier separating a carbonyl/hydroxyl overlap from its inverse (hydroxyl/carbonyl) should be no more than a couple of hundred reciprocal centimeters, so that a nonrigid space group isomorphic with $P2/m$ would provide a more apropriate description for this structure than $P2$.

This example of an additional element of symmetry being provided by a low-energy structural adjustment leads us to inquire whether there are any others available to this substance. The answer is a qualified yes: if a number of protons are cooperatively transferred from their hydroxyl oxygens to the carbonyl oxygens of the next unit cell (*e.g.*, from left to right in the top row of Figure 1b, from right to left in the bottom row) and electrons, skeletal atoms, and CF_3 groups are allowed to relax, a chain will result which is merely the original structure reflected in a plane normal to the chain axis. The nonrigid space group which includes this operation will be isomorphic with $P2_1/m$. The barrier for this operation is hard to estimate offhand, but it should certainly be no lower than the 1700 cm^{-1} hypothesized for a similar transfer within the CF_3COOH monomer.[25] Thus (if O/O overlapping is indeed present) the structure of solid CF_3COOH can be represented by a hierarchy of symmetry groups whose individual contributions will depend on the energy available to the system.

$$P2 \xrightarrow[\text{barrier} < 1 \text{ kcal/mol}]{\text{O/O puckering mode}} P2/m \xrightarrow[\text{barrier} > 5 \text{ kcal/mol}]{\text{cooperative proton transfer}} P2_1/m$$

Since the temperature at which $kT/hc = 1700$ cm^{-1} is around 2500°K, the extension to $P2_1/m$ will be unimportant except as a limiting case for techniques such as X-ray diffraction, where the position of the proton and the distinction between a carbonyl and a hydroxyl oxygen are not dominant. The temperature for which kT/hc is, say 150 cm^{-1}, however, is only 216°K, well below the melting point (258°K). It is thus possible that the phase transition at 220.5°K reported above represents the elimination of O/O overlap (the onset of free puckering), though of course other explanations (*e.g.*, the onset of free rotation of the CF_3 group) are available. The fact that the largest frequency differences over the phase change involve ν_{C-O} and δ_{COH} tends to support hypotheses involving the carboxyl groups.

Conclusions

(1) Neutron-scattering studies of liquid and solid CF_3COOH reported in the present work, considered in conjunction with earlier dielectric-constant[12,14] and spectroscopic[13,15] studies, indicate that this substance (in both states) is associated primarily in the form of hydrogen-bonded chains.

(2) Frequency differences between the infrared and Raman spectra of the solid indicate the presence of a center of symmetry in the unit cell. Of two simple structural models incorporating chains and a center of symmetry, one (monoclinic, $P2/m$) satisfactorily accommodates all experimental data presently available. The structural feature basic to this model is a double chain; its geometry suggests the presence of bifurcated hydrogen bonds.[16]

(3) Vibrational assignments for CF_3COOH and CF_3COOD in the region 2000–200 cm^{-1} are presented in Tables II and IV. Infrared, Raman, and neutron-scattering data[19] have been considered simultaneously in making the assignments, as have results from closely related molecules.[3,4] Observed interactions between vibrations which could not interact if the catemeric unit had a plane of symmetry suggest that such a plane is absent. A puckering of the catemeric unit about the carboxyl groups may be the rea on. This change formally reduces the space group to $P2$.

(4) Evidence has been found for the existence of a solid–solid phase transition in CF_3COOH at 220.5°K. Spectroscopic data suggest that the rearrangement involves the carboxyl groups. Definitive results on the structure of the solid and the nature of the transition cannot be obtained spectroscopically, of course, and will be available only after the necessary diffraction studies have been carried out.

(5) The region 910–610 cm^{-1} in the infrared spectrum of CF_3COOD is difficult to interpret, and evidently involves a change in the nature of the normal modes compared with CF_3COOH. This may or may not involve a change in the potential function around the hydroxyl group on deuteration (a normal-coordinate analysis must be carried out before even a tentative answer to this question can be obtained). Taylor and Templeton's observation[27] of different heats of dissociation for the deuterated and undeuterated gas-phase dimers indicates that a change in the potential function may well occur. In addition, Costain and Srivastava[28] found significant differences in the O···O distances of deuterated and undeuterated bimolecules formed from trifluoroacetic and formic acid. Spectroscopic studies of chromous acid[29] and monomeric acetic acid[30] have provided evidence for changes in the potential functions on deuteration of these compounds.

Acknowledgments. I am extremely grateful to Dr.

(27) M. D. Taylor and M. B. Templeton, *J. Amer. Chem. Soc.*, **78**, 2950 (1956).
(28) C. C. Costain and G. P. Srivastava, *J. Chem. Phys.*, **41**, 1620 (1964).
(29) R. G. Snyder and J. A. Ibers, *J. Chem. Phys.*, **36**, 1356 (1962).
(30) C. V. Berney, R. L. Redington, and K. C. Lin, *ibid.*, **53**, 1713 (1970).

B. C. G. Haywood for sharing his original neutron-scattering data and to Dr. Richard E. Miller for help with the Raman equipment and for hospitality at Michigan State University. Infrared spectra used in this study were obtained at the University of New Hampshire. Drs. Alan Cormier, Lynda Beck, and Don Spickerman have made significant contributions to various experimental aspects of this work. I thank Drs. S. F. Trevino and H. J. Prask for help and guidance in taking the spectra shown in Figure 2.

Electronic and Electron Spin Resonance Spectroscopic Study of the Sensitized Decomposition of Formaldehyde

Tuvia Bercovici and Ralph S. Becker*

Contribution from the Department of Chemistry, University of Houston, Houston, Texas 77004. *Received June 21, 1972*

Abstract: The sensitized decomposition of formaldehyde to formyl radical was examined using triphenylamine (TPA) and primarily in dichloromethane, in 3-methylpentane, and on silica gel at 77°K. The formation of formyl radical is monophotonic in dichloromethane and primarily biphotonic in 3-methylpentane and on silica gel. We propose (1) the monophotonic process occurs *via* energy transfer from the first excited singlet state of TPA and an excimer or exciplex may be involved and (2), the biphotonic process occurs *via* energy transfer from an upper excited triplet state, T_2 or greater, of TPA and an excimer or exciplex may be involved. Another mechanism could also exist in these cases. The disappearance of formyl radical apparently occurs *via* both second- and first-order processes. A solvent radical of dichloromethane is produced in the presence of formaldehyde and a mechanism is proposed for its formation.

The absorption spectrum of formyl radical in the visible region has been detected by Herzberg and Ramsay[1] in the flash photolysis of acetaldehyde in the gas phase. Pimentel, *et al.*,[2] studied the infrared absorption spectrum of formyl radical, obtained by the photolysis of HI in CO at 20°K. From the same method of obtaining the formyl radical, Adrian and Cochran[3,4] studied the esr spectrum. Marx and Chachaty[5] obtained the formyl radical by γ, X, and uv irradiation of solid formaldehyde at 77°K. Other methods have been used as the irradiation of water–methanol solutions at 77°K[6] or crystals of formic acid.[7]

In a recent work, McQuigg and Calvert[8] studied the photodecomposition of formaldehyde by flash photolysis. Two distinct primary photodissociative processes have been found in the photolysis of formaldehyde. The authors found that the relative quantum efficiencies of the two processes show a marked dependence on the wavelength of absorbed light. From this work and others,[9] it is concluded that the upper limit of D_{HCO-H} is 81.5–85 kcal/mol.

Prior to the present work, the formyl radical has not been obtained *via* energy transfer from a donor to formaldehyde. In addition, the present work discusses the reactions in terms of (1) the monophotonic *vs.* the biphotonic dependence upon the nature of the solvent, (2) the concentration and temperature dependence, (3) the nature and role of donor and solvent radicals, and (4) the mechanisms.

Experimental Section

Purified paraformaldehyde from Fisher Scientific Co. that had been dryed 2 days in a vacuum desiccator over sulfuric acid was used. Formaldehyde was prepared in either of two ways. Formaldehyde gas formed from the decomposition of paraformaldehyde in mineral oil (at 120–140°) was passed through a $CaCl_2$ tube, together with nitrogen as carrier, directly into the appropriate solvent. The other method followed that described by Spence and Wild.[10]

Phillips Petroleum Co. pure grade 3-methylpentane (3-MP) was distilled of Na–Pb alloy and passed over dryed neutral silica gel and then over a silica gel–silver nitrate column. Fisher methylene chloride (reagent grade) and pure Eastman Organic Chemicals Co. triphenylamine (TPA) were used without further purification.

For photoreactions of TPA on silica gel, the experiment was conducted as follows: 12 mg of TPA in 5 ml of 3-MP was added to 1 g of silica gel; the mixture was evaporated and dried under vacuum for 1 day. From this was taken 0.4 g and formaldehyde was distilled onto the mixture as described in the literature.[11] Solutions of TPA and formaldehyde were obtained as follows: in an esr sample tube, 0.4 ml of a solution of TPA (2.5 mg in 1 cc of 3-MP) was added, the solvent vacuum evaporated, and formaldehyde distilled onto the TPA.

Solutions of formaldehyde in high concentrations ($>5 \times 10^{-2}$ *M*) in 3-MP are not stable at room temperature.[11] For this reason, cooling needs to be done very quickly for reproducible results.

Absorption spectra were taken on a Cary 15 recording spectrophotometer. The emission spectra were determined by the front-face method as described by Becker, *et al.*[12] Epr determinations were conducted in a Varian (E-3) epr spectrometer, and all irradiations were conducted with a 100-W high-pressure mercury lamp.

(1) G. Herzberg and D. A. Ramsay, *Proc. Roy. Soc., Ser. A*, **233**, 34 (1955).
(2) G. E. Erwin, W. E. Thompson, and G. C. Pimentel, *J. Chem. Phys.*, **32**, 927 (1960).
(3) F. J. Adrian, E. L. Cochran, and V. A. Bowers, *ibid.*, **36**, 1661 (1962).
(4) E. L. Cochran, F. J. Adrian, and V. A. Bowers, *ibid.*, **44**, 4626 (1966).
(5) R. Marx and M. C. Chachaty, *ibid.*, **58**, 527 (1961).
(6) J. A. Brivati, N. Keen, and M. C. R. Symons, *J. Chem. Soc.*, 237 (1962).
(7) R. W. Holmberg, *J. Chem. Phys.*, **51**, 3255 (1969).
(8) R. D. McQuigg and J. G. Calvert, *J. Amer. Chem. Soc.*, **91**, 1590 (1969).
(9) E. Murad and M. G. Inghram, *J. Chem. Phys.*, 41, 404 (1964).
(10) R. Spence and W. Wild, *J. Chem. Soc.*, 338 (1935).
(11) T. Bercovici, J. King, and R. S. Becker, *J. Chem. Phys.*, **56**, 3956 (1972).
(12) R. S. Becker, E. Dolan, and D. E. Balke, *ibid.*, **50**, 239 (1969).